Track-to-Track Fusion Configurations and Association in a Sliding Window

XIN TIAN

YAAKOV BAR-SHALOM

Track-to-track fusion (T2TF) is very important in distributed tracking systems. Compared to the centralized measurement fusion (CMF), T2TF can be done at a lower rate and thus has potentially lower communication requirements. In this paper we investigate the optimal T2TF algorithms under linear Gaussian (LG) assumption, which can operate at an arbitrary rate for various information configurations. It is also assumed that the tracking system is synchronized. Namely, all the trackers obtain measurements and do track updates simultaneously and there are no communication delays between local trackers and the fusion center (FC). The algorithms presented in this paper can be generalized to asynchronous scenarios. First, the algorithms for T2TF without memory (T2TFwoM) are presented for three information configurations: with no, partial and full information feedback from the FC to the local trackers. As one major contribution of this paper, the impact of information feedback on fusion accuracy is investigated. It is shown that using only the track estimates at the fusion time (T2TFwoM), information feedback will have a negative impact on the fusion accuracy. Then, the algorithms for T2TF with memory (T2TFwM), which are optimal at an arbitrary rate, are derived for configurations with no, partial and full information feedback. It is shown that, operating at full rate, T2TFwM is equivalent to the CMF regardless of information feedback. However, at a reduced rate, a certain amount of degradation in fusion accuracy is unavoidable. In contrast to T2TFwoM, T2TFwM benefits from information feedback.

For nonlinear distributed tracking systems, an approximate implementation of the T2TF algorithms is proposed. It requires less communications between the FC and the local trackers, which allows the algorithms to be implemented in distributed tracking systems with low communication capacity. Simulation results show that the proposed approximate implementation is consistent and has practically no loss in fusion accuracy due to the approximation. For the sensors-target geometry considered, it can meet the performance bound of the CMF at the fusion times.

The problem of track-to-track association (T2TA) is also investigated. The sliding window test for T2TA, which uses track estimates within a time window, is derived. It accounts exactly for the crosscovariances among the track estimates and yields false alarm rates that match the theoretical values. To evaluate the test power when using more data frames, a comparison between the single time association test and the sliding window test is performed. Counterintuitively, it is shown that the belief "the longer the window, the greater the test power" is not always correct.

Manuscript received January 4, 2008; revised January 2, 2009; released for publication September 4, 2009.

Refereeing of this contribution was handled by Chee-Yee Chong.

Authors' address: Dept. of Electrical and Computer Engineering, University of Connecticut, Storrs CT 06269-2157, E-mail: ({xin.tian, ybs}@engr.uconn.edu).

1557-6418/09/$17.00

1. INTRODUCTION

In a multisensor tracking system, the fusion center (FC) is meant to gather and process information from local sensors or trackers. There are generally two approaches for this purpose. One is the centralized measurement fusion (CMF), in which the local measurements are sent directly to the FC, where the central tracker performs measurement to track association and track update. The other approach is track-to-track fusion (T2TF) in which local tracks are sent to the FC where tracks of the same target are fused for improved accuracy. In this paper, each track is assumed to be generated by a Kalman filter, which is optimal under linear Gaussian (LG) assumption and the same as the linear minimum mean square error (LMMSE) estimator for linear systems without the Gaussian assumption. It is also assumed that the tracking system is synchronized. Namely, all the trackers obtain measurements and perform track updates simultaneously and there are no communication delays between local trackers and the FC. The T2TF algorithms presented in this paper can be generalized to asynchronous cases which will be discussed in [26]. Although the CMF approach produces the best results, it requires constant and reliable communication links between local senors and the FC. Lags in the communication links will result in out-of-sequence measurements (OOSM), thus requiring special algorithms [2]. If the communication links become saturated because there are too many measurements to transmit, the sensor network will lose information and might fail. The T2TF approach is more attractive for practical implementations. It allows the local trackers to communicate with the FC once in a while, sending local tracks for T2TF and possibly receiving as feedback the fused tracks from the FC. The major benefit is that there is no restriction on when and how often the local tracks should be transmitted. This can reduce the requirements on the capacity of the communication links.

For the problem of T2TF, the crosscorrelation among tracks of the same target due to common process noises was first observed in [1], where a formula for the calculation of the crosscovariance was also presented. Based on the formula in [1], the algorithm for the one-scan T2TF, i.e., T2TF without memory (T2TFwoM) was studied in [5], which derived the algorithm for T2TFwoM without information feedback (T2TFwoMnf) at an arbitrary rate (see also [17, 18, 19, 20, 21, 22, 27]). Another type of T2TF algorithm—the information matrix fusion (IMF)—was proposed in [13, 25]. Note that, unlike T2TFwoM, the IMF belongs to the class of fuser with memory, since it uses track estimates from the previous fusion. The IMF is equivalent to the CMF when the fuser is operating at full rate [9, 13]. Comparisons between the IMF and the T2TFwoMnf can be found in [8, 9], where it is shown that, operating at full rate, the T2TFwoMnf is not as accurate as the IMF, and it was concluded that the suboptimality of

T2TFwoMnf is because it is optimal only in ML sense.[1] However, the IMF is not optimal when the fuser is operating at reduced rate and, as reported in [10], it causes inconsistency and even divergence. A simulation based comparison on existing fusion algorithms can also be found in [23].

In this paper, the T2TF algorithms that can operate at an arbitrary rate are investigated for various information configurations:

1. T2TFwoMnf (T2TFwoM with no information feedback)
2. T2TFwoMpf (T2TFwoM with partial information feedback)
3. T2TFwoMff (T2TFwoM with full information feedback)
4. T2TFwMnf (T2TFwM with no information feedback)
5. T2TFwMpf (T2TFwM with partial information feedback)
6. T2TFwMff (T2TFwM with full information feedback)

Except for T2TFwoMnf presented in [5], the results for all the other configurations are new. The impact of information feedback and memory on the accuracy of T2TF is thoroughly examined.

For T2TFwoM, depending on the existence of information feedback, the three information configurations [6, 15] are illustrated in Fig. 1. Suppose there are two tracks (that pertain to the same target) which are fused at certain times. The first configuration is the T2TFwoM without information feedback (T2TFwoMnf) [3], designated as Type IIa configuration for multisensor tracking in [6]. As indicated in Fig. 1(a), the two local tracks evolve independently without the information from each other, thus the improved accuracies are achieved only at the fusion times at the FC. The second configuration is the T2TFwoM with partial information feedback (T2TFwoMpf) which belongs to the Type IIb configuration in [6]. In this case, as shown in Fig. 1(b), track 1 is fused with track 2 and continues with the fused track (feedback) from the FC. However, track 2 does not receive the fused track in view of the partial information feedback. The third configuration is the T2TFwoM with full information feedback (T2TFwoMff), which also belongs to the Type IIb configuration in [6]. As shown in Fig. 1(c), both local trackers receive and continue with the fused track.

As shown in this paper T2TFwoM has a degradation in fusion accuracy compared to the CMF, and information feedback has a negative impact on the fusion accuracy of T2TFwoM. However the degradation in fusion accuracy of T2TwoM can be recovered by using also the track estimates from the previous fusion. Accordingly,

[1]The actual reason that T2TFwoMnf is (slightly) inferior to IMF operating at full rate (when it is algebraically equivalent to CMF, see [6] Section 8.6) is the lack of memory of T2TwoMnf. This is discussed in detail in Section 2.4 and Section 3.4.

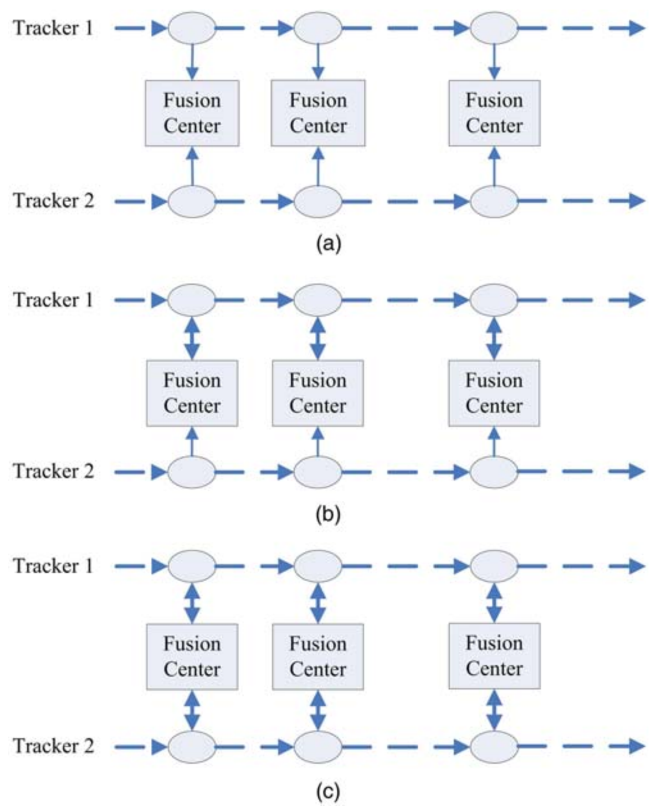

Fig. 1. Information configurations for T2TFwoM (horizontal axis is time). (a) T2TFwoM with no feedback. (b) T2TFwoM with partial feedback (Fusion Center to Tracker 1). (c) T2TFwoM with full feedback (Fusion Center to Tracker 1 and Tracker 2).

the algorithms for T2TFwM are derived for configurations with no, partial and full information feedback. It is shown that, when operating at full rate, T2TFwM is equivalent to the CMF (which is the global optimum) regardless of information feedback. However, at reduced rate, a certain amount of loss in fusion accuracy is unavoidable, and in contrast to the case of T2TFwoM, information feedback improves the fusion accuracy of T2TFwM. Furthermore, unlike the IMF, the T2TFwM algorithms derived in this paper are optimal at any rate.

As pointed out in [8], the major difficulty for the practical implementation of the optimal T2TF algorithm is that it requires all the local filter gains and observation matrices since the last fusion. In nonlinear distributed tracking systems, the local information is not directly available at the FC. In view of this, we propose an approximate implementation of the T2TF algorithms. It is based on the idea of reconstructing local information at the FC with minimum amount of information from the local trackers, which has much less communication requirements than the transmission of those local matrices [12]. Simulation results show that this approximate implementation is consistent and has practically no loss in accuracy due to the approximation.

Studies on the problem of track-to-track association (T2TA) can be found in [4, 24], in which the tests for T2TA are made based on a single frame of data. In [16], it is claimed that the test based on an average of

TABLE I
List of Acronyms

CMF	Centralized Measurement Fusion	configuration IV
IMF	Information Matrix Fusion	special configuration II^{M}
T2TF	Track-to-Track Fusion	
T2TFwoM	Track-to-Track Fusion without memory	configuration II
T2TFwoMnf	T2TFwoM with no information feedback	configuration II_{nf}
T2TFwoMpf	T2TFwoM with partial information feedback	configuration II_{pf}
T2TFwoMff	T2TFwoM with full information feedback	configuration II_{ff}
T2TFwM	Track-to-Track Fusion with memory	configuration II^{M}
T2TFwMnf	T2TFwM with no information feedback	configuration $\text{II}^{\text{M}}_{\text{nf}}$
T2TFwMpf	T2TFwM with partial information feedback	configuration $\text{II}^{\text{M}}_{\text{pf}}$
T2TFwMff	T2TFwM with full information feedback	configuration $\text{II}^{\text{M}}_{\text{ff}}$

the single time tests within a time window has improved performance over the single time test. However, this conclusion was drawn ignoring the state errors' crosscorrelation in time [7]. In this paper the *chi-square based sliding window test for T2TA*, which uses track estimates within a time window, is derived. It accounts exactly for all the crosscovariances among the track estimates and yields false alarm rates that match the theoretical values. To evaluate the test power when using more data frames (longer window), a comparison between the single time test and the sliding window test is performed. Counterintuitively, it is shown that *the belief "the longer the window, the more the power" is not necessarily correct*. This is because the power of the test depends on both the noncentrality parameter and the degrees of freedom of the (chi-square) test statistic. When the multiple frames of data selected for T2TA are strongly correlated, which happens for motion with low process noises (because the filter has "longer memory" in this case), the gain in the noncentrality parameter by using more data frames is too small to overcome the negative impact of the increased degrees of freedom on the power of the test. Thus, the sliding window test may be counterproductive and has *lower power* than the single time test.

All the results presented are optimal under the LG assumption.[2] The paper is organized as follows. Section 2 discusses the algorithms for T2TFwoM with no, partial and full information feedback. Section 3 derives the algorithms for T2TFwM with no, partial and full information feedback and shows the impact of information feedback on T2TFwM. In Section 4, the approximate implementation of the T2TF algorithms is proposed and evaluated in a tracking scenario with a nonlinear measurement model. The problem of T2TA test is investigated in Section 5, where the sliding window test is derived and compared with the single time test. Section 6 summarizes the paper with conclusions. For the convenience of readers, Table I lists the acronyms used in this paper and extends the configurations discussed in [6].

2. TRACK-TO-TRACK FUSION WITHOUT MEMORY (T2TFwoM) AT AN ARBITRARY RATE

This section investigates the algorithms of T2TFwoM (configuration II [6]) at an arbitrary rate. Section 2.1 formulates the problem. In Section 2.2 the T2TFwoM algorithms are presented for information configurations: with no, partial and full information feedback. Section 2.3 presents the simulation results that compare the fusion accuracies of T2TFwoMnf, T2TFwoMpf, T2TFwoMff and CMF. This leads to the observation that, in T2TFwoM, information feedback will cause a degradation of the fusion accuracy. This phenomenon is further explained in Section 2.4.

2.1. Problem Formulation: T2TFwoM

Consider the basic scenario with two local trackers (designated as 1 and 2) at different locations. Each tracker obtains measurements with its local sensor and maintains local tracks of the targets. For the sake of simplicity, it is assumed that the system operates in a synchronous fashion, where all the trackers obtain measurements and do local track updates simultaneously with sampling interval T. Communication links, which have no delay in time, are available between the FC and the local trackers. Each local tracker is allowed to communicate with the FC once in a while, sending its tracks to the FC and possibly receiving the fused tracks (when there is information feedback). At the FC, the fusion of the tracks of a target from trackers 1 and 2 is formulated as follows.[3] Let $\hat{x}_1(k \mid k)$, $P_1(k \mid k)$ and $\hat{x}_2(k \mid k)$, $P_2(k \mid k)$ represent the two local tracks at the fusion time. Assuming the crosscovariance of the two tracks $P_{12}(k \mid k)$ is available at the FC, T2TFwoM should be performed, so that

$$[\hat{x}_c(k \mid k), P_c(k \mid k)] = \mathbf{f}[\hat{x}_1(k \mid k), P_1(k \mid k), \hat{x}_2(k \mid k), P_2(k \mid k), P_{12}(k \mid k)] \tag{1}$$

where $\hat{x}_c(k \mid k)$ and $P_c(k \mid k)$ represent the fused track. After the fusion, the local tracks and their crosscovariance should also be updated to $\hat{x}_1^*(k \mid k)$, $P_1^*(k \mid k)$, $\hat{x}_2^*(k \mid k)$,

[2]In the case of fusion the algorithms presented constitute the LMMSE fuser, also called BLUE in, e.g., [18].

[3]Association (see [6] Section 8.4) is assumed to have been already performed.

$P_2^*(k \mid k)$ and $P_{12}^*(k \mid k)$ according to the information configuration of the fusion (possible feedback from the FC). Throughout the paper, superscript "$*$" is used to indicate post-fusion tracks. Note that (1) implies that only the local track estimates at the fusion time are used for T2TFwoM, i.e., this is a fuser without memory of fused and local track estimates from the previous fusion time.[4]

2.2. The Algorithms for T2TFwoM

If the local tracks $\hat{x}_1(k \mid k)$, $P_1(k \mid k)$, $\hat{x}_2(k \mid k)$, $P_2(k \mid k)$ and their crosscovariance $P_{12}(k \mid k)$ are available at the FC, the optimal[5] T2TFwoM can be done according to Eqs. (8.4.4-4)–(8.4.4-5) in [6], namely,

$$\begin{aligned}\hat{x}_c(k \mid k) &= \hat{x}_1(k \mid k) + [P_1(k \mid k) - P_{12}(k \mid k)] \\ &\quad \cdot [P_1(k \mid k) + P_2(k \mid k) - P_{12}(k \mid k) - P_{21}(k \mid k)]^{-1} \\ &\quad \cdot [\hat{x}_2(k \mid k) - \hat{x}_1(k \mid k)] \\ &= \hat{x}_1(k \mid k) + K_{12}(k)[\hat{x}_2(k \mid k) - \hat{x}_1(k \mid k)] \end{aligned} \tag{2}$$

$$\begin{aligned}P_c(k \mid k) &= P_1(k \mid k) - [P_1(k \mid k) - P_{12}(k \mid k)] \\ &\quad \cdot [P_1(k \mid k) + P_2(k \mid k) - P_{12}(k \mid k) - P_{21}(k \mid k)]^{-1} \\ &\quad \cdot [P_1(k \mid k) - P_{21}(k \mid k)] \end{aligned} \tag{3}$$

where

$$P_{12}(k \mid k) = P_{21}(k \mid k)' = \mathrm{Cov}[\tilde{x}_1(k \mid k), \tilde{x}_2(k \mid k)]. \tag{4}$$

To calculate $P_{12}(k \mid k)$, suppose the previous fusion was performed at discretized time l, after which one has the errors

$$\tilde{x}_1^*(l \mid l) = \hat{x}_1^*(l \mid l) - x(l) \tag{5}$$

$$\tilde{x}_2^*(l \mid l) = \hat{x}_2^*(l \mid l) - x(l) \tag{6}$$

where $x(l)$ denotes the true state of the target at l. Let

$$P_1^*(l \mid l) = \mathrm{Cov}[\tilde{x}_1^*(l \mid l), \tilde{x}_1^*(l \mid l)] \tag{7}$$

$$P_2^*(l \mid l) = \mathrm{Cov}[\tilde{x}_2^*(l \mid l), \tilde{x}_2^*(l \mid l)] \tag{8}$$

$$P_{12}^*(l \mid l) = \mathrm{Cov}[\tilde{x}_1^*(l \mid l), \tilde{x}_2^*(l \mid l)]. \tag{9}$$

From Eq. (8.4.2-2) in [6], one has

$$\begin{aligned}\tilde{x}_s(l+1 \mid l+1) &= [I - K_s(l+1)H_s(l+1)]F(l)\tilde{x}_s(l \mid l) \\ &\quad - [I - K_s(l+1)H_s(l+1)]v(l) \\ &\quad + K_s(l+1)w_s(l+1) \qquad s = 1,2. \end{aligned} \tag{10}$$

Using (10) recursively for both the cental and local tracks from discrete time l to k, it follows that

$$\begin{aligned}\tilde{x}_s(k \mid k) &= W_s^e(k,l)\tilde{x}_s^*(l \mid l) + \sum_{i=l+1}^{k} W_s^v(k,i-1)v(i-1) \\ &\quad + \sum_{i=l+1}^{k} W_s^w(k,i)w_s(i), \qquad s = 1,2 \end{aligned} \tag{11}$$

where the weights are defined as

$$W_s^e(k,l) = \prod_{i=0}^{k-l-1} [I - K_s(k-i)H_s(k-i)]F(k-i-1) \tag{12}$$

$$\begin{aligned}W_s^v(k,i-1) &= -\left\{\prod_{j=0}^{k-i-1} [I - K_s(k-j)H_s(k-j)]F(k-j-1)\right\} \\ &\quad \cdot [I - K_s(i)H_s(i)] \end{aligned} \tag{13}$$

and

$$W_s^w(k,i) = \left\{\prod_{j=0}^{k-i-1} [I - K_s(k-j)H_s(k-j)]F(k-j-1)\right\} K_s(i) \tag{14}$$

in which $K_s(i)$, $i = l+1,\ldots,k$ are the Kalman filter gains and $H_s(i)$ are the observation matrices at local tracker s and $F(i-1)$ are the state transition matrices. Eq. (11) is the expression of the errors of the tracks from Kalman filters as weighted sums of the previous error at a certain point and the intervening process and measurement noises. The significance of this expression is that it shows explicitly all the sources of uncertainty and provides the general tool for the derivations of the T2TF and T2TA algorithms in the absence or presence of memory and feedback.

From (11) and the whiteness assumption of the measurement noises and the process noises, the crosscovariance $P_{12}(k \mid k)$, required by the T2TFwoM given in (2)–(3), can be calculated as

$$\begin{aligned}P_{12}(k \mid k) &= W_1^e(k,l)P_{12}^*(l \mid l)W_2^e(k,l)' \\ &\quad + \sum_{i=l+1}^{k} W_1^v(k,i-1)Q(i-1)W_2^v(k,i-1)' \end{aligned} \tag{15}$$

where $Q(i)$ is the covariance of the process noises at time i. Similarly to (11), the error of the fused track (2) can be expressed as

$$\begin{aligned}\tilde{x}_c(k \mid k) &= \tilde{x}_1(k \mid k) + K_{12}(k)[\tilde{x}_2(k \mid k) - \tilde{x}_1(k \mid k)] \\ &= [I - K_{12}(k)]\tilde{x}_1(k \mid k) + K_{12}(k \mid k)\tilde{x}_2(k \mid k). \end{aligned} \tag{16}$$

[4]A fuser with memory (of the previous track estimates) uses the track estimates from the previous fusion time, which, as shown in Section 3.4, improves fusion accuracy.

[5]MMSE if all the estimation errors are Gaussian and LMMSE otherwise [7].

After the fusion, local tracks 1 and 2 and their crosscovariance should be updated according to the information configuration.

In configuration T2TFwoMnf (see Fig. 1(a)), one has

$$\hat{x}_1^*(k \mid k) = \hat{x}_1(k \mid k) \tag{17}$$

$$P_1^*(k \mid k) = P_1(k \mid k) \tag{18}$$

$$\hat{x}_2^*(k \mid k) = \hat{x}_2(k \mid k) \tag{19}$$

$$P_2^*(k \mid k) = P_2(k \mid k) \tag{20}$$

$$P_{12}^*(k \mid k) = P_{12}(k \mid k) \tag{21}$$

where $P_{12}(k \mid k)$ is given in (15).

In configuration T2TFwoMpf (see Fig. 1(b))

$$\hat{x}_1^*(k \mid k) = \hat{x}_c(k \mid k) \tag{22}$$

$$P_1^*(k \mid k) = P_c(k \mid k) \tag{23}$$

$$\hat{x}_2^*(k \mid k) = \hat{x}_2(k \mid k) \tag{24}$$

$$P_2^*(k \mid k) = P_2(k \mid k) \tag{25}$$

and according to (16)

$$P_{12}^*(k \mid k) = [I - K_{12}(k)]P_{12}(k \mid k) + K_{12}(k)P_2(k \mid k). \tag{26}$$

In configuration T2TFwoMff (see Fig. 1(c))

$$\hat{x}_2^*(k \mid k) = \hat{x}_1^*(k \mid k) = \hat{x}_c(k \mid k) \tag{27}$$

$$P_2^*(k \mid k) = P_1^*(k \mid k) = P_c(k \mid k) \tag{28}$$

$$P_{12}^*(k \mid k) = P_c(k \mid k). \tag{29}$$

The algorithm of T2TFwoM is summarized as follows:

- At the FC, the local tracks are fused according to (2)–(3).
- The fusion can be done exactly, if the following data are available:
  (i) The local tracks to be fused: $\hat{x}_1(k \mid k)$, $P_1(k \mid k)$ and $\hat{x}_2(k \mid k)$, $P_2(k \mid k)$
  (ii) The covariances and crosscovariance from the previous fusion at time l: $P_1^*(l \mid l)$, $P_2^*(l \mid l)$, $P_{12}^*(l \mid l)$ (see (7)–(8))—needed for the calculation of the current crosscovariance.
  (iii) The local weights (12)–(13).
- Depending on the information configuration, the local tracks are updated accordingly using (17)–(21) for T2TFwoMnf, or (22)–(26) for T2TFwoMpf, or (27)–(29) for T2TFwoMff.

The algorithm of T2TFwoM has no theoretical limit on the number of the local trackers. Only the crosscovariances among all the tracks of the same target need to be properly calculated. See [11] for the n-sensors version of the fusion equations (2)–(3). The use of the results from [11] in the general case requires Eqs. (11)–(13) for each sensor.

TABLE II
Fuser Variances (at fusion times) in Steady State
(fusion interval: 5 s)

Fusion Type	FC Track at Fusion Time	
	Pos	Vel
T2TFwoMff	133	6.29
T2TFwoMpf	131	6.30
T2TFwoMnf	125	6.30
CMF	119	6.03

2.3. Comparison of the T2TFwoM Algorithms and the CMF

The algorithms for T2TFwoM are evaluated first in the following tracking scenario. The target state is defined as $[x\ \dot{x}]'$. The target motion is modeled as the discrete white noise acceleration (DWNA) model in [7], Section 6.3.2. It is assumed that two sensors obtain position measurements of the target with a sampling interval of $T = 1$ s. The standard deviation of the measurement noise is $\sigma_w = 30$ m and the process noise variance is $q = 1\ \mathrm{m}^2/\mathrm{s}^4$. T2TFwoM takes place every 5 s, i.e., at a reduced rate.

All the fusers are consistent in the simulations (their covariance calculations are exact). In view of the consistency, the performance comparison can be made using the calculated covariances. Table II shows the steady state variances of position and velocity at the FC. All the fused tracks are more accurate than the single-sensor (local) tracks without fusion, which have steady state variances as 205 in position and 7.26 in velocity. Note that at the fusion time the position estimates of all the fused tracks have a small degradation compared to the CMF: 5% for T2TFwoMnf, 10% for T2TFwoMpf, 12% for T2TFwoMff. This shows that T2TFwoM has a degradation in fusion accuracy compared to the CMF and the degradation increases in the presence of information feedback. This apparently counterintuitive result is further discussed in the next subsection.

2.4. The Impact of Information Feedback on T2TFwoM

To show the impact of information feedback on T2TFwoM, consider the following two-step scalar estimation problem. At time 0, two local estimators have independent prior information: $\bar{x}_1 \sim N(x(0), P_1)$ at estimator 1 and $\bar{x}_2 \sim N(x(0), P_2)$ at estimator 2. At time 1, $x(1) = x(0) + v_1$ where the process noise $v_1 \sim N(0, Q)$. The estimators have independent measurements of the state: $z_1 = x(1) + w_1$ ($w_1 \sim N(0, R_1)$) at estimator 1 and $z_2 = x(1) + w_2$ ($w_2 \sim N(0, R_2)$) at estimator 2. The errors in the prior information, the process noise and the measurement noises are all independent. For the sake of simplicity it is assumed that $P_1 = P_2 = R_1 = R_2 = 1$ and $Q = 1/2$. Consider the fusion at time 1 and the fuser uses only the track estimates at time 1, namely T2TFwoM. Fig. 2 shows the information flow of the centralized

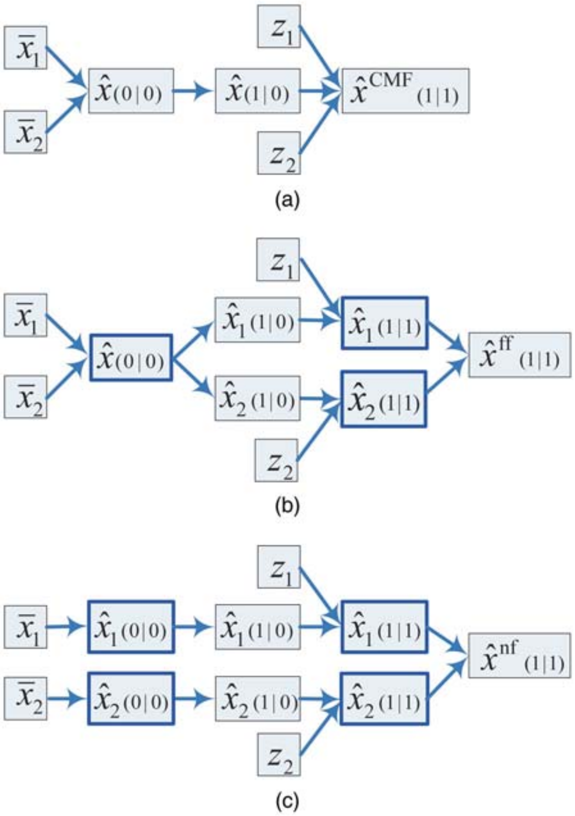

Fig. 2. Information flow (CMF and T2TFwoM). (a) CMF (configuration IV). (b) T2TFwoMff (configuration IIff). (c) T2TFwoMnf (configuration IInf).

measurement fusion (CMF), T2TFwoM with full information feedback (T2TFwoMff) and T2TFwoM with no information feedback (T2TFwoMnf). Note that in T2TFwoMff the information feedback (sharing) occurs at time 0 in this example.

Using CMF (Configuration IV in Section 8.2.5 of [6]), one has

$$\hat{x}^{\mathrm{CMF}}(1 \mid 1) = \tfrac{1}{6}\bar{x}_1 + \tfrac{1}{6}\bar{x}_2 + \tfrac{1}{3}z_1 + \tfrac{1}{3}z_2 \tag{30}$$

with error (using the weighted sum form)

$$\tilde{x}^{\mathrm{CMF}}(1 \mid 1) = \tfrac{1}{6}\tilde{x}_1 + \tfrac{1}{6}\tilde{x}_2 - \tfrac{1}{3}v_1 + \tfrac{1}{3}w_1 + \tfrac{1}{3}w_2 \tag{31}$$

where $\tilde{x}_1$ and $\tilde{x}_2$ denote the errors of $\bar{x}_1$ and $\bar{x}_2$. It is easy to calculate the covariance

$$\mathrm{Cov}[\hat{x}^{\mathrm{CMF}}(1 \mid 1)] = \tfrac{1}{3}. \tag{32}$$

In T2TFwoMff,[6] one has

$$\hat{x}^{\mathrm{ff}}(1 \mid 1) = \tfrac{1}{4}\bar{x}_1 + \tfrac{1}{4}\bar{x}_2 + \tfrac{1}{4}z_1 + \tfrac{1}{4}z_2 \tag{33}$$

with error

$$\tilde{x}^{\mathrm{ff}}(1 \mid 1) = \tfrac{1}{4}\tilde{x}_1 + \tfrac{1}{4}\tilde{x}_2 - \tfrac{1}{2}v_1 + \tfrac{1}{4}w_1 + \tfrac{1}{4}w_2 \tag{34}$$

[6]Note that, following Section 8.2.3 of [6], Configuration IIb does not have a memory of past estimates at the FC. It is T2TFwoM.

and

$$\mathrm{Cov}[\hat{x}^{\mathrm{ff}}(1 \mid 1)] = \tfrac{3}{8}. \tag{35}$$

In T2TFwoMnf (Configuration IIa in Section 8.2.3 [6]), it follows that

$$\hat{x}^{\mathrm{nf}}(1 \mid 1) = \tfrac{1}{5}\bar{x}_1 + \tfrac{1}{5}\bar{x}_2 + \tfrac{3}{10}z_1 + \tfrac{3}{10}z_2 \tag{36}$$

with error

$$\tilde{x}^{\mathrm{nf}}(1 \mid 1) = \tfrac{1}{5}\tilde{x}_1 + \tfrac{1}{5}\tilde{x}_2 - \tfrac{2}{5}v_1 + \tfrac{3}{10}w_1 + \tfrac{3}{10}w_2 \tag{37}$$

and

$$\mathrm{Cov}[\hat{x}^{\mathrm{nf}}(1 \mid 1)] = \tfrac{17}{50}. \tag{38}$$

Then one has

$$\mathrm{Cov}[\hat{x}^{\mathrm{CMF}}(1 \mid 1)] < \mathrm{Cov}[\hat{x}^{\mathrm{nf}}(1 \mid 1)] < \mathrm{Cov}[\hat{x}^{\mathrm{ff}}(1 \mid 1)]. \tag{39}$$

There are losses in accuracy in T2TFwoMff and T2TFwoMnf compared to the CMF, although they are relatively small, due to the large process noise in the example. Comparing (31), (34) and (37), it can be seen that the weights of the measurements are lower in T2TFwoMnf than in the CMF. They become even lower in T2TFwoMff due to the information feedback, which leads to the further loss in fusion accuracy.

3. THE ALGORITHMS FOR T2TFwM AT AN ARBITRARY RATE

The results in Section 2.4 show that, at full rate, T2TFwoM is less accurate than the CMF and information feedback is detrimental to T2TFwoM. However, the IMF is equivalent to the CMF when operating at full rate [13]. In this case, T2TFwoM is inferior to the IMF. This is because T2TFwoM uses only local estimates at the fusion time, which contain most but not all of the information for T2TF. In contrast, the IMF belongs to the class of T2TFwM. However, at *reduced rate*, the IMF algorithm is not optimal anymore.

To account for the information from the fused and local track estimates from the previous fusion time,[7] the algorithm for T2TFwM at an *arbitrary rate* is derived in the next three subsections for configurations with no, partial and full information feedback, designated as T2TFwMnf, T2TFwMpf and T2TFwMff respectively. Fig. 3 shows the information flow of the three configurations.

3.1. The Algorithm for T2TFwMnf

As shown in Fig. 3(a), for T2TFwMnf, at fusion time k, the track estimates to be fused are local track

[7]This implies one-step memory. In fact, there is no need for more, since one-step memory summarizes, under the LG (or LMMSE) assumptions, all the information from the previous track estimates. This is confirmed by the simulation results in Section 3.4, which show that, at full rate, T2TFwM (using one-step memory) yields the globally optimal fusion results.

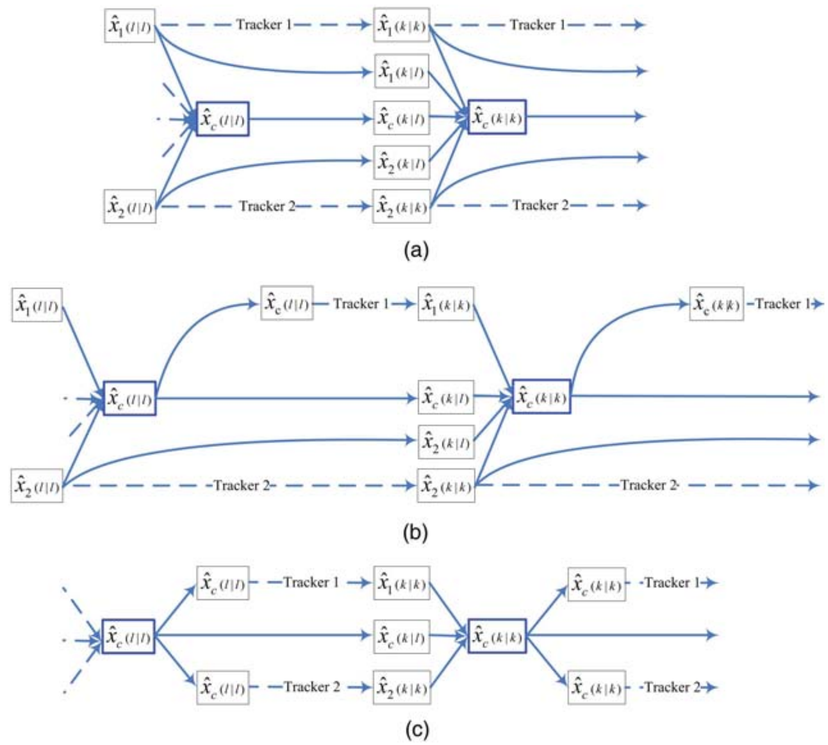

Fig. 3. Information flow: T2TFwM at an arbitrary rate. (a) T2TFwM with no information feedback (one cycle: from fusion time l to the next fusion time k). (b) T2TFwM with partial information feedback (one cycle: from fusion time l to the next fusion time k). (c) T2TFwM with full information feedback (one cycle: form fusion time l to the next fusion time k).

estimates $\hat{x}_1(k \mid k)$, $\hat{x}_2(k \mid k)$ and the predicted track estimates $\hat{x}_1(k \mid l)$, $\hat{x}_2(k \mid l)$ and $\hat{x}_c(k \mid l)$ from the previous fusion, where subscript "c" indicates the (fused) track at the FC. Stacking the estimates and the predicted estimates as a vector, one has

$$\mu = [\hat{x}_1(k \mid k) \quad \hat{x}_2(k \mid k) \quad \hat{x}_c(k \mid l) \quad \hat{x}_1(k \mid l) \quad \hat{x}_2(k \mid l)]'. \tag{40}$$

The fusion of these track estimates requires the covariance of μ, denoted as $\mathrm{Cov}(\mu)$. To obtain this covariance, a slight modification of (11) gives

$$\tilde{x}_s(k \mid l) = W_0^e(k,l)\tilde{x}_s^*(l \mid l) + \sum_{i=l+1}^{k} W_0^v(k,i-1)v(i-1) \tag{41}$$

where $s = 1,2,c$ and

$$W_0^e(k,l) = \prod_{i=0}^{k-l-1} F(k-i-1) \tag{42}$$

$$W_0^v(k,i-1) = -\prod_{j=0}^{k-i-1} F(k-j-1) \tag{43}$$

which are obtained by substituting the filter gains $K_s(i)$ in (12) and (13) by zero matrices, since the filter gains are zero in the predicted track estimates. From (12), (13), (42) and (43), $\mathrm{Cov}(\mu)$ can be easily calculated with linear algebra.

For T2TFwMnf, define the following difference matrix

$$M = \begin{bmatrix} I & 0 & -I & 0 & 0 \\ 0 & I & -I & 0 & 0 \\ 0 & 0 & -I & I & 0 \\ 0 & 0 & -I & 0 & I \end{bmatrix} \tag{44}$$

where I denotes identity matrix of appropriate dimension, such that

$$\nu = \begin{bmatrix} \hat{x}_1(k \mid k) - \hat{x}_c(k \mid l) \\ \hat{x}_2(k \mid k) - \hat{x}_c(k \mid l) \\ \hat{x}_1(k \mid l) - \hat{x}_c(k \mid l) \\ \hat{x}_2(k \mid l) - \hat{x}_c(k \mid l) \end{bmatrix} = M\mu. \tag{45}$$

Using the standard MMSE estimator from [7], the fused estimate is given by

$$\hat{x}_c(k \mid k) = \hat{x}_c(k \mid l) + \mathrm{Cov}[x(k),\nu]\mathrm{Cov}(\nu)^{-1}\nu \tag{46}$$

where $x(k)$ is the true state of the target at time k, and

$$\mathrm{Cov}[x(k),\nu] = -[\mathrm{Cov}(\mu)]_{(3,:)}M' \tag{47}$$

$$\mathrm{Cov}(\nu) = M\mathrm{Cov}(\mu)M' \tag{48}$$

where $[\mathrm{Cov}(\mu)]_{(i,:)}$ denotes the ith row of matrix $\mathrm{Cov}(\mu)$. In (46) $\hat{x}_c(k \mid l)$ plays the role of the prior at the FC and the other elements of μ play the role of the observations.

From (45)–(48), the fused estimate is

$$\hat{x}_c(k \mid k) = \hat{x}_c(k \mid l) - [\mathrm{Cov}(\mu)]_{(3,:)} M'(M\mathrm{Cov}(\mu)M')^{-1} M\mu$$
$$= \hat{x}_c(k \mid l) + K_\mu \mu \quad (49)$$

where

$$K_\mu \triangleq -[\mathrm{Cov}(\mu)]_{(3,:)} M'(M\mathrm{Cov}(\mu)M')^{-1} M. \quad (50)$$

The fused covariance is

$$P_c(k \mid k) = P_c(k \mid l) - \mathrm{Cov}[x(k),\nu]\mathrm{Cov}(\nu)^{-1}\mathrm{Cov}[x(k),\nu]'$$
$$= P_c(k \mid l) - [\mathrm{Cov}(\mu)]_{(3,:)} M'(M\mathrm{Cov}(\mu)M')^{-1} M \cdot [[\mathrm{Cov}(\mu)]_{(3,:)}]'$$
$$= P_c(k \mid l) + K_\mu [[\mathrm{Cov}(\mu)]_{(3,:)}]'. \quad (51)$$

For T2TFwMnf the crosscovariances between the fused track and the tracks from trackers 1 and 2 can be obtained from (49) as

$$P_{1c}(k \mid k) \triangleq \mathrm{Cov}[\hat{x}_1(k \mid k), \hat{x}_c(k \mid k)]$$
$$= [\mathrm{Cov}(\mu)]_{(1,3)} + [\mathrm{Cov}(\mu)]_{(1,:)} K'_\mu \quad (52)$$
$$P_{2c}(k \mid k) \triangleq \mathrm{Cov}[\hat{x}_2(k \mid k), \hat{x}_c(k \mid k)]$$
$$= [\mathrm{Cov}(\mu)]_{(2,3)} + [\mathrm{Cov}(\mu)]_{(2,:)} K'_\mu \quad (53)$$

where $[\mathrm{Cov}(\mu)]_{(i,j)}$ is element (i,j) of $\mathrm{Cov}(\mu)$.

Since there is no information feedback, both local tracks are not changed after the fusion is performed at the FC. One has

$$\hat{x}_1^*(k \mid k) = \hat{x}_1(k \mid k) \quad (54)$$
$$P_1^*(k \mid k) = P_1(k \mid k) \quad (55)$$
$$\hat{x}_2^*(k \mid k) = \hat{x}_2(k \mid k) \quad (56)$$
$$P_2^*(k \mid k) = P_2(k \mid k) \quad (57)$$
$$P_{12}^*(k \mid k) = P_{12}(k \mid k) \quad (58)$$
$$P_{1c}^*(k \mid k) = P_{1c}(k \mid k) \quad (59)$$
$$P_{2c}^*(k \mid k) = P_{2c}(k \mid k). \quad (60)$$

3.2. The Algorithm for T2TFwMpf

Unlike T2TFwMnf, in T2TFwMpf, one has $\hat{x}_1(k \mid l) = \hat{x}_c(k \mid l)$. Consequently, the elements $\hat{x}_1(k \mid l)$ in (40) should be removed. In this case, redefine μ in (40) and M in (44) as

$$\mu = [\hat{x}_1(k \mid k) \quad \hat{x}_2(k \mid k) \quad \hat{x}_c(k \mid l) \quad \hat{x}_2(k \mid l)]' \quad (61)$$

and

$$M \triangleq \begin{bmatrix} I & 0 & -I & 0 \\ 0 & I & -I & 0 \\ 0 & 0 & -I & I \end{bmatrix}. \quad (62)$$

It follows that

$$\nu = \begin{bmatrix} \hat{x}_1(k \mid k) - \hat{x}_c(k \mid l) \\ \hat{x}_2(k \mid k) - \hat{x}_c(k \mid l) \\ \hat{x}_2(k \mid l) - \hat{x}_c(k \mid l) \end{bmatrix} = M\mu. \quad (63)$$

Then, similarly to T2TFwMnf, the fused estimate $\hat{x}_c(k \mid k)$ is obtained using (49) and the fused covariance $P_c(k \mid k)$ follows from (51) using the modified definitions (61) and (62).

After the fusion, the local tracks and the track crosscovariances are updated as follows

$$\hat{x}_1^*(k \mid k) = \hat{x}_c(k \mid k) \quad \text{(feedback)} \quad (64)$$
$$P_1^*(k \mid k) = P_c(k \mid k) \quad \text{(feedback)} \quad (65)$$
$$P_{1c}^*(k \mid k) = P_c(k \mid k) \quad \text{(feedback)} \quad (66)$$
$$\hat{x}_2^*(k \mid k) = \hat{x}_2(k \mid k) \quad \text{(no feedback)} \quad (67)$$
$$P_2^*(k \mid k) = P_2(k \mid k) \quad \text{(no feedback)} \quad (68)$$
$$P_{12}^*(k \mid k) = P_{2c}(k \mid k)' \quad (69)$$
$$P_{2c}^*(k \mid k) = P_{2c}(k \mid k) \quad (70)$$

where $P_{2c}(k \mid k)$ is given by (53) using the modified definitions (61) and (62).

3.3. The Algorithm for T2TFwMff

In contrast to T2TFwMnf, in T2TFwMff, one has $\hat{x}_1(k \mid l) = \hat{x}_2(k \mid l) = \hat{x}_c(k \mid l)$. Consequently, the elements $\hat{x}_1(k \mid l)$ and $\hat{x}_2(k \mid l)$ in (40) should be removed. In this case, redefine μ in (40) and M in (44) as

$$\mu = [\hat{x}_1(k \mid k) \quad \hat{x}_2(k \mid k) \quad \hat{x}_c(k \mid l)]' \quad (71)$$

and

$$M = \begin{bmatrix} I & 0 & -I \\ 0 & I & -I \end{bmatrix}. \quad (72)$$

It follows that

$$\nu = \begin{bmatrix} \hat{x}_1(k \mid k) - \hat{x}_c(k \mid l) \\ \hat{x}_2(k \mid k) - \hat{x}_c(k \mid l) \end{bmatrix} = M\mu. \quad (73)$$

Then, similarly to T2TFwMnf, the fused estimate is obtained using (49) and the fused covariance follows from (51) using the modified definitions (71) and (72).

Due to full information feedback, the local tracks and the track crosscovariances are updated as

$$\hat{x}_1^*(k \mid k) = \hat{x}_c(k \mid k) \quad \text{(feedback)} \quad (74)$$
$$P_1^*(k \mid k) = P_c(k \mid k) \quad \text{(feedback)} \quad (75)$$
$$P_{1c}^*(k \mid k) = P_c(k \mid k) \quad \text{(feedback)} \quad (76)$$
$$\hat{x}_2^*(k \mid k) = \hat{x}_c(k \mid k) \quad \text{(feedback)} \quad (77)$$
$$P_2^*(k \mid k) = P_2(k \mid k) \quad \text{(feedback)} \quad (78)$$
$$P_{12}^*(k \mid k) = P_{2c}^*(k \mid k) = P_c(k \mid k) \quad \text{(feedback)}. \quad (79)$$

Note that in T2TFwMff the crosscovariances between the fused track and the local tracks after the information feedback are the same with the fused covariance (51). This is different from the updated crosscovariances in T2TFwMnf, i.e., (59) and (60).

TABLE III
Fuser and Tracker 1 Calculated Variances at Fusion Times for $N_f = 1$ (full rate), $q = 0.3$, $R_1 = R_2 = 1$

Time		1	2	3	4	5	6
T2TFwMnf	Tracker 1	1.0000	0.5652	0.4639	0.4331	0.4230	0.4196
	Fuser	0.5000	0.3077	0.2743	0.2673	0.2658	**0.2654**
T2TFwMpf	Fuser	0.5000	0.3077	0.2743	0.2673	0.2658	**0.2654**
T2TFwMff	Fuser	0.5000	0.3077	0.2743	0.2673	0.2658	**0.2654**
CMF		0.5000	0.3077	0.2743	0.2673	0.2658	**0.2654**

TABLE IV
Fuser and Tracker 1 Calculated Variances at Fusion Times for $N_f = 3$ (reduced rate), $q = 0.3$, $R_1 = R_2 = 1$

Time		1	3	6	9	12	15
T2TFwMnf	Tracker1	1.0000	0.4639	0.4196	0.4180	0.4179	0.4179
	Fuser	0.5000	0.2772	0.2698	0.2694	0.2694	**0.2694**
T2TFwMpf	Fuser	0.5000	0.2763	0.2690	0.2688	0.2688	**0.2688**
T2TFwMff	Fuser	0.5000	0.2755	0.2683	0.2682	0.2682	**0.2682**
CMF		0.5000	0.2743	0.2654	0.2653	0.2653	**0.2653**

3.4. Performance Comparison: T2TFwMnf vs. T2TFwMff and CMF

To evaluate the performance of the optimal T2TF with memory (T2TFwM) at an arbitrary rate, consider the following tracking scenario. The state of the target (taken as a scalar for simplicity) evolves according to

$$x(k) = x(k-1) + v(k), \qquad k = 2,3,\ldots \tag{80}$$

where $v(k)$ is the process noise with variance q.

There are two trackers, 1 and 2, taking measurements of the target with measurement noises w_1 and w_2, namely,

$$z_i(k) = x(k) + w_i(k), \qquad i = 1,2 \tag{81}$$

where $w_i(k)$ are zero-mean Gaussian noises with variance R_i. The two trackers calculate tracks of the target with their own measurements using a Kalman filter. Each local track is initialized at time 1 with the first local measurement. The first T2TF happens at time 1. Then T2TFwM occurs every N_f sampling times.

Table III shows the fuser- and tracker-calculated variances of the errors of the track estimates when the fuser is operating at full rate. It can be seen that, at full rate, the fuser with memory (with no, partial and full information feedback) is equivalent to the CMF.

Table IV shows the fuser- and tracker-calculated variances when the fuser (with memory) is operating at reduced rate. In this case, T2TFwM, with or without information feedback, has a small loss in fusion accuracy compared to the CMF. This is because, in T2TF, information from the common process noises and the common prior information (due to information feedback) appears simultaneously in different local tracks, which causes their weights (and, consequently, also the weights of the new measurements) in the fused track to deviate from the global optimum. This is similar to the T2TFwoM example discussed in Section 2.4. When T2TFwM is done at full rate, these deviations are fully corrected by fusing the previous track estimates (see [6], Section 8.6). However, at a lower rate, the deviations can not be fully corrected, thus, a certain amount of degradation in fusion accuracy is unavoidable. Also note that, in contrast to the case of T2TFwoM, T2TFwMff is more accurate than T2TFwMpf and T2TFwMnf, namely information feedback *improves* fusion accuracy in T2TFwM (as expected). While it is too involved to provide a theoretical proof of this result, simulations in different settings confirm this.

Another fusion algorithm that also uses the previous track estimates (i.e., it has memory) is the IMF [13, 25]. When operating at full rate, the IMF is algebraically equivalent to the CMF (see [6], Section 8.6) and also to the algorithms for T2TFwM presented in this section. However, at a lower rate, the IMF is not an optimal algorithm. As reported in [10], this may even lead to divergence. In contrast, the algorithms for T2TFwMnf, T2TFwMpf and T2TFwMff are optimal at any rate.

3.5. Summary of the Various T2TF Configurations

To summarize the discussion in Section 2 and Section 3:

- For T2TFwoM (which uses only the track estimates at the fusion time), information feedback will cause a degradation in fusion accuracy (see Section 2.4). This is because the local trackers use locally optimal but globally suboptimal filter gains, which leads to lower gains for the new measurements in the fused track.

TABLE V
Data Required from Local Tracker 2 for each Fusion with Fusion Interval of M

	Data Required	The Total Amounts (bits)
Exact algorithm	$W_2^e(k,l)$, $W_2^v(k,i-1)$, $\hat{x}_2$, P_2	$[(M+1)n_x^2 + n_x + 0.5(n_x+1)n_x]n_{\text{acc}}$
Approximate algorithm	Measurement time stamps, $\hat{x}_2$, P_2	$Mn_T + [n_x + 0.5(n_x+1)n_x]n_{\text{acc}}$

n_{acc}: The number of the bits for each element in the state and covariance (accuracy)
n_x: Dimension of the state n_T: The number of bits for each measurement time stamp

Information feedback will lower the gains further, and cause more degradation in fusion accuracy.

- The algorithms for T2TFwM (which uses also the track estimates from the previous fusion) at an arbitrary rate for different information configurations (with and without information feedback) are derived for the first time. When operating at full rate, T2TFwM, with no, partial or full information feedback, is equivalent to the CMF (global optimum). When operating at a reduced rate, T2TFwMnf, T2TFwMpf and T2TFwMff all have a small degradation in fusion accuracy compared to the CMF. However, unlike the case of T2TFwoM, the degradation is smaller for T2TFwMff than for T2TFwMpf and T2TFwMnf. Namely information feedback improves fusion accuracy in T2TFwM.

4. THE APPROXIMATE IMPLEMENTATION OF THE T2TF ALGORITHMS

The T2TF algorithms at an arbitrary rate require the local weight matrices (12)–(13) at the FC. However, transmission of these matrices might not be affordable in practical distributed tracking systems due to limit in communication capacity. The idea of the approximate implementation is to approximately reconstruct the local information required by the T2TF algorithms at the FC using a minimum amount of information from the local trackers. Section 4.1 presents the approximate implementation which has significantly lower communication requirements than the original algorithms. Simulation results in Section 4.2 show that this implementation is consistent and has practically no loss in the fusion accuracy due to the approximation.

4.1. The Approximate Algorithm

Note that the local weighting matrices (12)–(13) are functions of $F(i-1)$, $H_s(i)$, $K_s(i)$, $i = l+1,\ldots,k$. At the FC, if estimates of the target positions (i.e., an approximate trajectory of the target) are available, using also the locations of the local sensors and the times when the local measurements are taken, the observation matrices used by the local tracker and the related track updates can be approximately reconstructed, yielding $\bar{H}_s(i)$, $\bar{K}_s(i)$, $i = l+1,\ldots,k$. Note that these reconstructions do not need the actual measurements due to the nature of the Kalman filter that the covariance updates do not depend on the actual measurements. Thus the approximate evaluation of (12)–(13) is given by[8]

$$\bar{W}_s^e(k,l) = \prod_{i=0}^{k-l-1}[I - \bar{K}_s(k-i)\bar{H}_s(k-i)]F(k-i-1) \tag{82}$$

$$\bar{W}_s^v(k,i-1) = -\left\{\prod_{j=0}^{k-i-1}[I - \bar{K}_s(k-j)\bar{H}_s(k-j)]F(k-j-1)\right\} \cdot [I - \bar{K}_s(i)\bar{H}_s(i)] \tag{83}$$

where overbar denotes the approximate values. For T2TF, (15) can be approximated by

$$\bar{P}_{12}(k \mid k) = \bar{W}_1^e(k,l)P_{12}^*(l \mid l)\bar{W}_2^e(k,l)' + \sum_{i=l+1}^{k}\bar{W}_1^v(k,i-1)Q(i-1)\bar{W}_2^v(k,i-1)'. \tag{84}$$

Thus, to approximately calculate the local weights (12)–(13) required in the T2TF algorithms, the FC needs to know the following: (i) the locations of the local sensors, (ii) the time when the local measurements are obtained (considering the possibility of missed detections in practical systems) and (iii) an approximate trajectory of the target. Note that, at the FC, (iii) is available when there is a tracker running at the FC or it can be obtained by interpolation between the track estimates at the fusion times. Although extra computations are required at the FC to obtain the approximate weights at the local trackers, these computations are affordable due to the simplicity of the expressions involved. A brief analysis of the savings in communication is given below.

In distributed tracking systems with sensors at fixed locations, there is no need to transmit the locations. Assume further that tracker 1 is collocated with the FC and, thus, the approximate track trajectory can be obtained from its track estimates. Table V compares the amount of data that needs to be transmitted from local tracker 2 to the FC in the exact algorithm and in

[8]If the measurements are linear (as in [18]) there is no need for this approximation. In the problem considered later, the measurements are nonlinear (range and azimuth); consequently, this approximation will be needed.

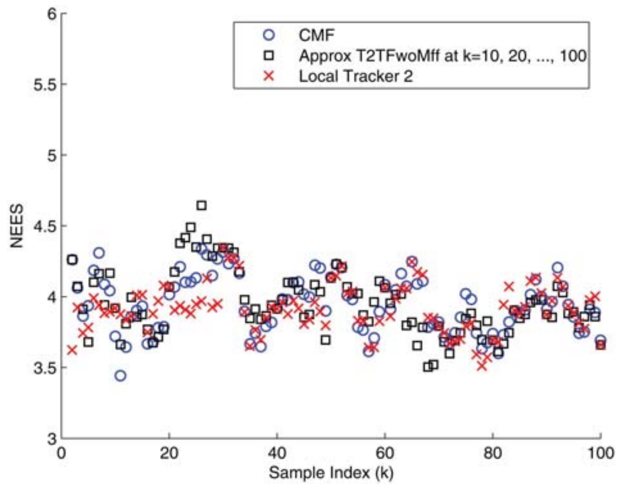

Fig. 4. Filter consistency test: NEES (T2TFwoMff).

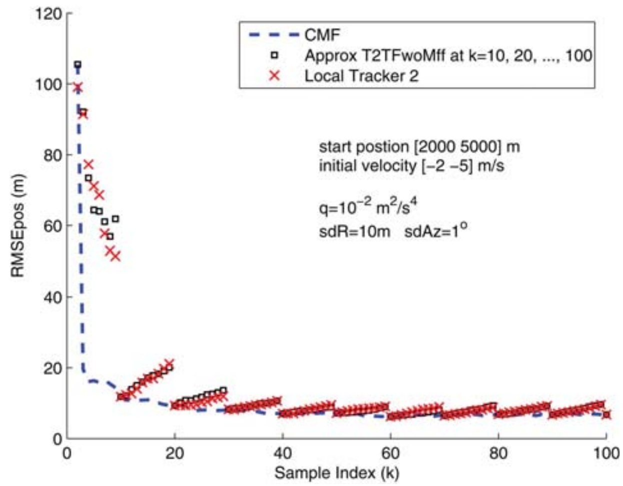

Fig. 5. RMS position errors (T2TFwoMff).

the approximate implementation. Given that transmission of measurement time stamps is much less expensive than transmission of the local weights, namely, $(M+1)n_x^2 n_{\text{acc}} \gg M n_T$, the savings in communication using the approximate algorithm is significant.

4.2. Simulation Results

The approximate implementation of the T2TF algorithms is tested in a 2-D multisensor tracking scenario, in which one target is tracked by two trackers. The target motion is modeled as a DWNA process [7] with process noise variance q. The target state is defined as $x = [\xi\ \dot{\xi}\ \zeta\ \dot{\zeta}]'$. Tracker 1 is located at [0 0] m and tracker 2 is at [0 10000] m. The local sensors (radars) obtain position measurements of the target in their polar coordinates, namely, range and azimuth, every $T = 1$ s. The filter used by the trackers is the converted measurement Kalman filter (CMKF) [7]. It is assumed that tracker 1 is collocated with the FC, i.e., the FC has access to the estimates of tracker 1, and tracker 2 sends its track $(\hat{x}_2(k \mid k), P_2(k \mid k))$ to the FC every 10 sampling intervals. The simulation results are obtained from 100 Monte-Carlo (MC) runs.

4.2.1. T2TFwoM with full Information Feedback (T2TFwoMff)

Figs. 4–5 show the performance of the approximate implementation in the case of T2TFwoMff. As shown in Fig. 4, the fused tracks are always consistent (the normalized estimation error squared (NEES)) are in their 95% probability region [3.46 4.69]). In Fig. 5, significant improvement in track accuracies from both trackers is observed at the fusion times $k = 10, 20, \ldots, 100$. The results of the CMF are also presented as the bound of the tracking performance. The root mean square (RMS) position errors indicate that the fused track practically meets the performance bound of the CMF at the fusion times. Between the fusion times the errors increase because each tracker is on its own. The loss of accuracy because of the information feedback in the fused track (discussed in Section 2.3) becomes insignificant due to the geometric diversity of the two tracks.[9] The results for velocity are similar. Since the approximate implementation performs practically as well as the CMF, there is no need in this case to evaluate the exact algorithm for T2TFwoMff.

4.2.2. T2TFwoM with Partial Information Feedback (T2TFwoMpf)

Figs. 6–7 show the performance of the approximate implementation in the case of T2TFwoMpf for the same tracking scenario with the following modification: tracker 2 does not receive the fused track from the FC. Fig. 6 shows that the fused track is consistent. In terms of achieved accuracy, it also meets the performance bound of the CMF at the fusion points.

4.2.3. The Effect of Ignoring the Crosscovariance in T2TFwoMff

Figs. 8–9 show the statistics from the same tracking scenario, but the T2TFwoMff is performed assuming that the two tracks are uncorrelated. The divergence of the filter—very rapid in NEES, slower but noticeable in RMSE—demonstrates the importance of taking into account the crosscovariances. This happens because the excessive optimism (fused covariances that are too small) due to ignoring the crosscovariances.

[9] With the two sensors widely separated (10000 m apart in the simulation), and the measurements much more accurate in the range direction than the crossrange direction, the two tracks are geometrically complementary to each other in the scenario considered. In such cases, the improvements of accuracy of the fused track are very significant, and they are less affected by the crosscorrelation between the tracks.

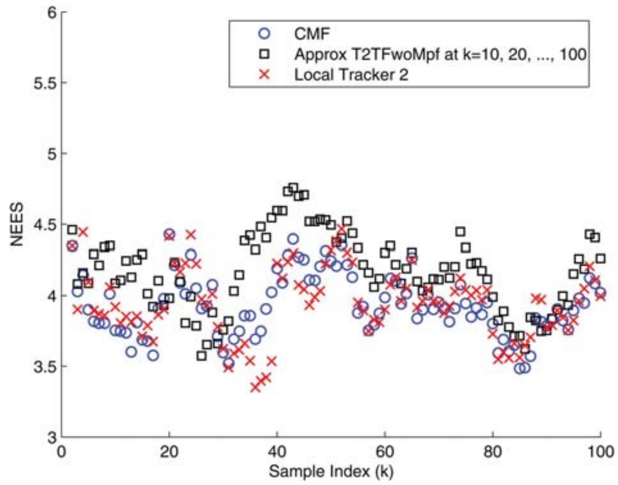

Fig. 6. Filter consistency test: NEES (T2TFwoMpf).

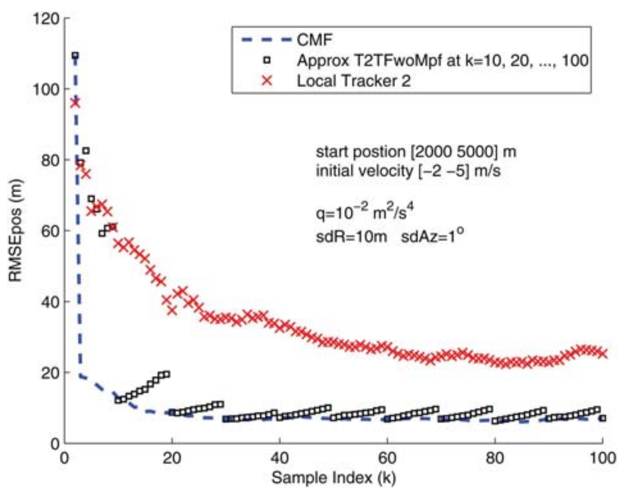

Fig. 7. RMS position errors (T2TFwoMpf).

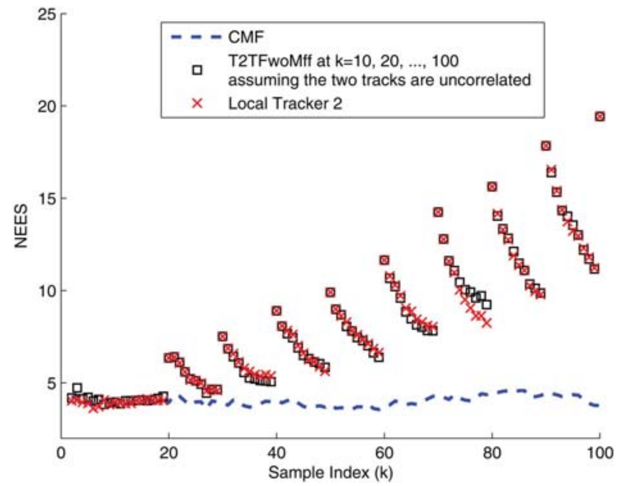

Fig. 8. Filter consistency test: NEES (T2TFwoMff). Ignoring the crosscovariances in T2TFwoMff leads to divergence.

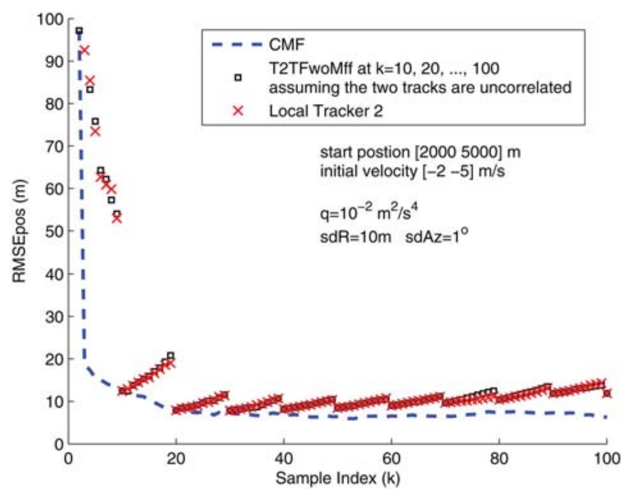

Fig. 9. RMS position errors (T2TFwoMff).

5. SLIDING WINDOW TEST FOR T2TA

The chi-square based track-to-track association (T2TA) test is investigated in this section. Note that the chi-square based T2TA test is based only on the likelihood function (LF) under H_0 (the two tracks belong to the same target). The optimal (likelihood ratio—LR) test can not be used for T2TA, since the exact LF under H_1 (the two tracks do not belong to the same target) is not available. Although a diffuse prior may be used to calculate the LF under H_1, which leads to a LR test that is the same as the chi-square based test. The test still has virtually no information about H_1.[10] The test can be done based on a single frame of track estimates, or using track estimates at multiple times. Conventional belief is that, given the same false alarm rate, using multiple frames of data will yield higher power. Accordingly the sliding window test is proposed in Section 5.1, which is shown to yield false alarm rates that match the theoretical values. Then we compare the power of the sliding window test to that of the single time test. Counterintuitively, it is observed that the sliding window test, which uses more data, does not necessarily have more power than the single time test. The reason for this phenomenon is discussed in Section 5.2.

5.1. The Algorithm of the Sliding Window Test for T2TA

Consider the basic T2TA test of whether two tracks originated from the same target. For the single time test at time k, the data includes the tracks $\hat{x}_1(k \mid k)$, $P_1(k \mid k)$ from tracker 1 and $\hat{x}_2(k \mid k)$, $P_2(k \mid k)$ from tracker 2, as well as their crosscovariance $P_{12}(k \mid k)$. Define

$$\Delta(k) = \hat{x}_1(k \mid k) - \hat{x}_2(k \mid k). \tag{85}$$

It follows that

$$P_\Delta(k) = P_1(k \mid k) + P_2(k \mid k) - P_{12}(k \mid k) - P_{12}(k \mid k)' \tag{86}$$

[10]Also note that the chi-square based test uses only the Gaussian exponent (This has the disadvantage that large covariance leads to acceptance but it has low power). The assignment, however, will use the full LF, i.e., there is penalty for large covariance matrix.

where $P_{12}(k \mid k)$ is calculated from (15). The test statistic is

$$T(k) = \Delta(k)' P_\Delta(k)^{-1} \Delta(k) \qquad (87)$$

which, under H_0 (the two tracks are for the same target), is a random variable with a $\chi^2_{n_x}$ distribution (n_x is the dimension of the state). However, for data association at subsequent times, similar test statistics $T(g)$, $g > k$, are correlated with $T(k)$, thus the sum of single time test statistics (87) within a time window does not have a χ^2 distribution [4, 24].[11]

The sliding window test based on the most recent N frames of data needs to account for the crosscovariances among data at different times. Without loss of generality, consider the T2TA that occurs at time t_m. Define

$$\boldsymbol{\Delta}_N(t_m) = [\Delta(t_m) \quad \Delta(t_{m-1}) \ldots \Delta(t_{m-N+1})]' \qquad (88)$$

where subscript N is the window length and $\Delta(t_m), \ldots, \Delta(t_{m-N+1})$ are from the N most recent track estimates received by the FC. The test statistic $T_N(t_m)$ for this sliding window of N times is

$$T_N(t_m) = \boldsymbol{\Delta}_N(t_m)' \mathrm{Cov}[\boldsymbol{\Delta}_N(t_m)]^{-1} \boldsymbol{\Delta}_N(t_m) \qquad (89)$$

which, under H_0, has a χ^2 distribution with $N n_x$ degrees of freedom.

Given $\mathrm{Cov}[\boldsymbol{\Delta}_N(t_{m-1})]$ from the previous sliding window, to obtain $\mathrm{Cov}[\boldsymbol{\Delta}_N(t_m)]$, the new diagonal term

$$\mathrm{Cov}[\Delta(t_m)] = P_\Delta(t_m) \qquad (90)$$

is calculated from (86). The new off-diagonal terms are

$$\begin{aligned}
&\mathrm{Cov}[\Delta(t_m), \Delta(t_i)] \\
&\quad = \mathrm{Cov}[\tilde{x}_1(t_m \mid t_m) - \tilde{x}_2(t_m \mid t_m), \tilde{x}_1(t_i \mid t_i) - \tilde{x}_2(t_i \mid t_i)] \\
&\quad = \mathrm{Cov}[\tilde{x}_1(t_m \mid t_m), \tilde{x}_1(t_i \mid t_i)] + \mathrm{Cov}[\tilde{x}_2(t_m \mid t_m), \tilde{x}_2(t_i \mid t_i)] \\
&\qquad - \mathrm{Cov}[\tilde{x}_1(t_m \mid t_m), \tilde{x}_2(t_i \mid t_i)] - \mathrm{Cov}[\tilde{x}_2(t_m \mid t_m), \tilde{x}_1(t_i \mid t_i)], \\
&\qquad\qquad i = m - N + 1, \ldots, m - 1. \qquad (91)
\end{aligned}$$

From (11), it follows that

$$\begin{aligned}
\mathrm{Cov}[\Delta(t_m), \Delta(t_i)] &= W_e^1(t_m, t_i) P_1(t_i \mid t_i) + W_e^2(t_m, t_i) P_2(t_i \mid t_i) \\
&\quad - W_e^1(t_m, t_i) P_{12}(t_i \mid t_i) - W_e^2(t_m, t_i) P_{21}(t_i \mid t_i) \qquad (92)
\end{aligned}$$

where $P_1(t_i \mid t_i)$, $P_2(t_i \mid t_i)$ are from the tracks at time t_i and $P_{12}(t_i \mid t_i)$ is calculated using (15).

5.2. The Sliding Window Test vs. the Single Time Test

The sliding window test using test statistics (89) and the single time test with test statistics (87) are compared in a 1-D multisensor tracking scenario as in Section 2.3. Target 1 starts at 5000 m with an initial velocity −3 m/s. Target 2 starts at 5030 m with the same initial velocity (the initial target separation is 30 m).[12] Both targets have process noises with variance $q = 2 \cdot 10^{-2}$ m^2/s^4. These noises are independent across the targets, leading to their eventual separation. Two sensors, designated as 1 and 2, obtain position measurements of targets 1 and 2 every 1 s and maintain separate tracks for the targets. The T2TA tests are performed every 3 s, which is the time interval between two consecutive local track estimates used in the window test. The sliding window test uses a window of $N = 5$ times. For comparison, two tests based on the sum of the single time tests are also performed. One is the cumulative sum over all the previous single time tests; another is the sum of the single time tests within a sliding window of N as the approach proposed in [16, 24]. Both are not optimal because the correlations in time are ignored.

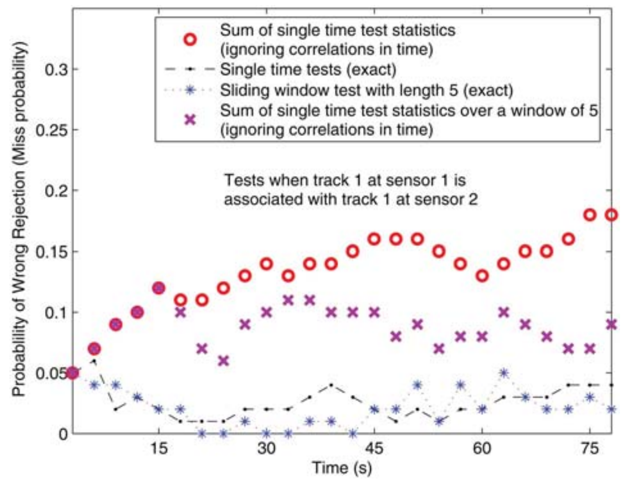

Fig. 10. Miss probability (wrong rejection) from 100 MC runs for 0.025 theoretical value (associations are done every 3 s).

Fig. 10 shows the miss probability when the track of target 1 at sensor 1 is associated with the track of the same target at sensor 2. The theoretical miss probability is 2.5% (correct acceptance 97.5%). The "single time test" (based on single frame of data) and the "sliding window test" match the theoretical error probability. However, the miss probabilities of the other two tests based on the sum of the single time test statistics are significantly larger than the theoretical value. This is due to the fact that these tests ignore the correlation among the single time test statistics.

Fig. 11 shows the probability of correct rejection (power of the test) for 0.025 miss probability when the track of target 1 at sensor 1 is associated with the track of target 2 at sensor 2. Surprisingly, the sliding window test has lower power than the single time test. This counterintuitive phenomenon is further analyzed in the Section 5.3 with an illustrative example.

[11]This is contrary to the assertion in [16].

[12]This small separation is only for the purpose of comparing the power of different tests for T2T association. It is assumed that these closely spaced targets are resolved by the sensors.

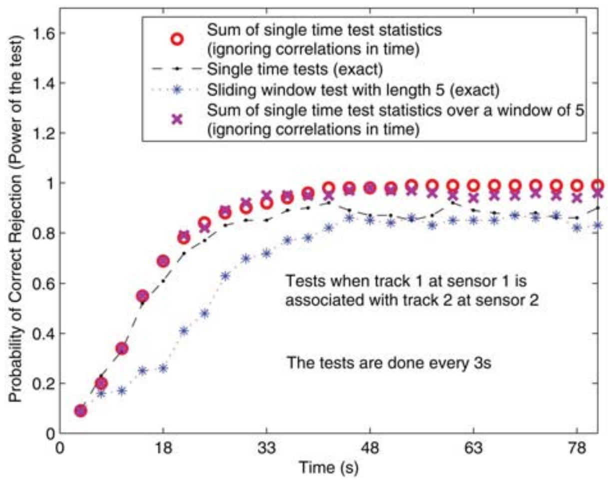

Fig. 11. Power of test for 0.025 miss probability from 100 MC runs.

5.3. The Effect of Window Length on the Power of the T2TA Test

Consider a scalar state estimation problem with two sensors/estimators. Estimator 1 has prior information $\hat{x}_1(0) \sim N(x_1(0), P_1)$, where $x_1(0)$ denotes the true state of the target corresponding to track 1 at time 0, P_1 is the variance of the estimate $\hat{x}_1(0)$. At time 1, this true state propagates to $x_1(1) = x_1(0) + v$ where $v \sim N(0, Q)$. A measurement is taken at time 1 as $z_1(1) = x_1(1) + w_1$, where $w_1 \sim N(0, R_1)$. Estimator 2 has prior information on the target corresponding to track 2, $\hat{x}_2(0) \sim N(x_2(0), P_2)$. At time 1, the state of this target evolves as $x_2(1) = x_2(0) + v$ and the measurement of sensor 2 is $z_2(1) = x_2(1) + w_2$, where $w_2 \sim N(0, R_2)$. It is assumed that the states of the two targets have the same process noise v, so the difference between their true states stays constant (they are moving in formation).[13] When the two targets are the same, $x_1(t) - x_2(t) = 0$, $t = 0, 1$, otherwise the target separation is $|x_1(t) - x_2(t)| = d > 0$, $t = 0, 1$. It is assumed that the errors in the prior information and the measurement noises are all independent and for the sake of simplicity $P_1 = P_2 = R_1 = R_2 = \sigma^2$.

For the T2TA test based on the prior information at time 0, one has

$$\Delta(0) = \hat{x}_1(0) - \hat{x}_2(0) \tag{93}$$

$$\mathrm{Var}[\Delta(0)] = P_1 + P_2 = 2\sigma^2 \tag{94}$$

$$T(0) = \mathrm{Var}[\Delta(0)]^{-1}\Delta(0)^2 = \frac{1}{2\sigma^2}\Delta(0)^2 \tag{95}$$

under H_0 (the two tracks are from the same target), $E[\Delta(0)] = 0$; under H_1 (the two tracks are from two different targets), $E[\Delta(0)] = d$.

At time 1, with the measurements z_1 and z_2, the updated estimates for the target (under H_0) or targets (under H_1) are

$$\hat{x}_1(1) = \frac{R_1}{P_1 + Q + R_1}\hat{x}_1(0) + \frac{P_1 + Q}{P_1 + Q + R_1}z_1 = \frac{\sigma^2}{2\sigma^2 + Q}\hat{x}_1(0) + \frac{\sigma^2 + Q}{2\sigma^2 + Q}z_1 \tag{96}$$

$$\hat{x}_2(1) = \frac{R_2}{P_2 + Q + R_2}\hat{x}_2(0) + \frac{P_2 + Q}{P_2 + Q + R_2}z_2 = \frac{\sigma^2}{2\sigma^2 + Q}\hat{x}_2(0) + \frac{\sigma^2 + Q}{2\sigma^2 + Q}z_2. \tag{97}$$

Thus

$$\Delta(1) = \hat{x}_1(1) - \hat{x}_2(1) = \frac{\sigma^2}{2\sigma^2 + Q}(\hat{x}_1(0) - \hat{x}_2(0)) + \frac{\sigma^2 + Q}{2\sigma^2 + Q}(z_1 - z_2) \tag{98}$$

$$\mathrm{Var}[\Delta(1)] = \frac{\sigma^4}{(2\sigma^2 + Q)^2}(P_1 + P_2) + \frac{(\sigma^2 + Q)^2}{(2\sigma^2 + Q)^2}(R_1 + R_2) = \frac{2Q^2\sigma^2 + 4Q\sigma^4 + 4\sigma^6}{(2\sigma^2 + Q)^2} \tag{99}$$

$$T(1) = \mathrm{Var}[\Delta(1)]^{-1}\Delta(1)^2 = \frac{(2\sigma^2 + Q)^2}{2Q^2\sigma^2 + 4Q\sigma^4 + 4\sigma^6}\Delta(1)^2 \tag{100}$$

under H_0, $E[\Delta(1)] = 0$ and under H_1, $E[\Delta(1)] = d$.

For the window test,

$$\boldsymbol{\Delta}_2(1) = [\Delta(0) \quad \Delta(1)]' \tag{101}$$

$$\mathrm{Cov}[\boldsymbol{\Delta}_2(1)] = \begin{bmatrix} 2\sigma^2 & \dfrac{2\sigma^4}{2\sigma^2 + Q} \\ \dfrac{2\sigma^4}{2\sigma^2 + Q} & \dfrac{2Q^2\sigma^2 + 4Q\sigma^4 + 4\sigma^6}{(2\sigma^2 + Q)^2} \end{bmatrix} \tag{102}$$

$$T_2(1) = \boldsymbol{\Delta}_2(1)'\{\mathrm{Cov}[\boldsymbol{\Delta}_2(1)]\}^{-1}\boldsymbol{\Delta}_2(1) \tag{103}$$

with $E[\boldsymbol{\Delta}_2(1) \mid H_0] = [0 \ \ 0]'$ and $E[\boldsymbol{\Delta}_2(1) \mid H_1] = [d \ \ d]'$.

Since the single time test is a special case of the window test with a window length of 1, $T(0)$ can also be denoted as $T_1(0)$ and $T(1)$ as $T_1(1)$. The tests statistics $T(0)$, $T(1)$ and $T_2(1)$, which are quadratic forms, have non-central Chi-square distributions with N degrees of freedom and noncentrality parameter λ [14]. The number of the degrees of freedom of the test statistic is the window length N and the noncentrality parameter λ is given by

$$\lambda_N(t) = E[\boldsymbol{\Delta}_N(t)]'\{\mathrm{Cov}[\boldsymbol{\Delta}_N(t)]\}^{-1}E[\boldsymbol{\Delta}_N(t)], \qquad t = 0, 1 \tag{104}$$

with the expectation taken conditioned on H_0 ("same target," i.e., $d = 0$) or H_1 ($d > 0$). Specifically,

$$T_N(t) \sim \chi^2(N, \lambda_N(t)), \qquad t = 0, 1. \tag{105}$$

[13] As later discussed, this assumption is necessary to obtain the actual theoretical performance of the test.

TABLE VI
Statistical Properties of the Test Statistics: Single Time Test vs. Sliding Window Test

Test statistic $\sim \chi^2(N,\lambda)$	Degrees of Freedom N	Noncentrality parameter λ	
		H_0	H_1
$T(0) = T_1(0)$	1	0	$\frac{1}{2\sigma^2}d^2$
$T(1) = T_1(1)$	1	0	$\frac{(2\sigma^2+Q)^2}{2Q^2\sigma^2+4Q\sigma^4+4\sigma^6}d^2$
$T_2(1)$	2	0	$\frac{1}{\sigma^2}d^2$

Notice that (105) holds only when the covariance matrices of $\boldsymbol{\Delta}_N(t)$ are the same under both H_0 and H_1, which requires the targets to have the same process noise. This happens when the targets move in formation. However, in general, different targets do not necessarily have the same process noise. In such cases, the test statistic $T_N(t)$ does not follow a non-central χ^2 distribution under H_1 and the difference between the true states of the targets is nonstationary. Thus the power of the test can not be obtained theoretically.

The cumulative distribution function (cdf) of a $\chi^2(N,\lambda)$ random variable is given by [28]

$$P\{\chi^2(N,\lambda)\leq x\} = \sum_{j=0}^{\infty} e^{\lambda/2}\frac{(\lambda/2)^j}{j!}\frac{\gamma(j+k/2,x/2)}{\Gamma(j+k/2)}. \tag{106}$$

Softwares are available for the calculation of (106).

The statistical properties of the above test statistics under H_0 and H_1 are shown in Table VI. Notice that, in this example, the noncentrality parameter of the window test $T_2(1)$ doesn't depend on the value of the process noise variance Q. This holds for this specific example but is not true in general. However, it is easy to show that the noncentrality parameter of the sliding window test is always greater than or equal to that of the single time test.

Assuming $\sigma^2 = 1$, Fig. 12 compares the noncentrality parameters for the window test ($N = 2$) and the single time test at time 1. It can be seen that, if $Q = 0$, then the noncentrality parameters of $T_2(1)$ and $T(1)$ are the same. However, $T_2(1)$ has 1 more degree of freedom than $T(1)$, thus the sliding window test $T_2(1)$ requires a higher threshold for the same miss probability of H_0 and, consequently, is less powerful than the single time test $T(1)$. As the variance of the process noise Q increases, the noncentrality parameter of $T_2(1)$ remains constant, and will be significantly larger than the noncentrality parameter of $T(1)$, which decreases with Q, as shown in Fig. 12. This compensates for the larger number of degrees of freedom of $T_2(1)$ and makes $T_2(1)$ eventually more powerful than $T(1)$.

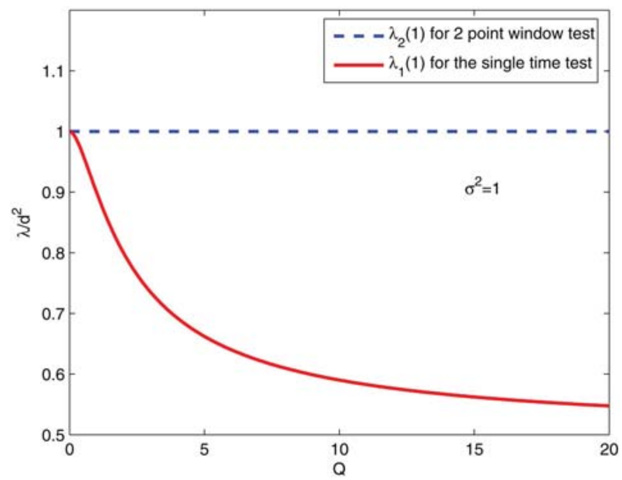

Fig. 12. The noncentrality parameters (normalized by the separation squared) vs. process noise variance.

Table VII compares the power of the tests under different process noise variances Q when $d = 3$ and $\sigma^2 = 1$. The "Threshold for rejection" and "Power of the test" are from the theoretical calculations. The "Miss probability" and "Correct rejection" are from Monte Carlo simulations and they match the theoretical values. The results show that when the process noise level is high ($Q = 6$), the window test has higher power than the single time test; however, counterintuitively, the window test has lower power than the single time test when the process noise level is low ($Q = 0.1$).

Note that the power of the test depends on (i) the number of degrees of freedom N of the chi-square

TABLE VII
Performance of the Tests ($d = 3$, $\sigma^2 = 1$ and Probability of Correct Acceptance $1-\alpha = 0.975$). Q is the Process Noise Variance; N is the Degrees of Freedom of the Test Statistic and λ is the Noncentrality Parameter. The Miss Probability and Correct Rejection (power) are Obtained form 1000 Monte Carlo (MC) Runs.

Test Stat	Q	N	λ under H_1	Threshold (rejection of H_0, $\alpha = 0.025$)	Theoretical power of the test	MC Miss Prob of H_0	MC Correct Rejection of H_0
$T(1)$	0.1	1	8.98	5.02	**0.775**	0.026	0.76
$T_2(1)$		2	9	7.38	**0.678**	0.030	0.69
$T(1)$	6	1	5.76	5.02	***0.56***	0.031	0.57
$T_2(1)$		2	9	7.38	***0.678***	0.029	0.66

test statistic (which determines the threshold) and (ii) the noncentrality parameter λ. Two explanations from different perspectives to this seemingly counterintuitive phenomenon are given next.

1. In this example, the power of the window test $T_2(1)$ remains the same over different process noise levels Q as a result of the constant noncentrality parameter, i.e., the window test is not sensitive to process noise levels. When the process noise level is low ($Q = 0.1$ in this example) the power of the single time test is higher than the window test's because it has almost the same noncentrality parameter as the window test but only one degree of freedom (i.e., lower threshold). However, with a high level of process noise (when $Q = 6$) the noncentrality parameter decreases and the power of the single time test drops below that of the window test.
2. At time 1, by incorporating the data from time 0, the window test has a noncentrality parameter larger than that of the single time test (for both cases when $Q = 0.1$ and $Q = 6$). However, the inclusion of the data from time 0 also increases the degrees of freedom of the test statistic (from 1 to 2), which has a negative impact on the power of the test (for the same false alarm rate, this raises the threshold to 7.38 from 5.02 for the single time test). When the crosscorrelation between the data at time 1 and time 0 is large (which happens for low process noise $Q = 0.1$), the increase in the noncentrality parameter is too small to overcome the negative effect of the increased degree of freedom. In such cases, the window test has lower power than the single time test.

The discussion above indicates that the advantage of the window is negated by the crosscorrelation in time, which is higher for low process noise.[14] This suggests that, to enhance the power of the sliding window test, it is necessary to make sure that the multiple frames of data selected for the test are not strongly correlated. This can be accomplished by increasing the time difference between the selected frames.

To confirm this guideline, Fig. 13 shows the power of the tests under a theoretical false alarm rate of $\alpha = 0.025$ in the same simulation scenario as in Section 5.2 except that the tests for T2TA are done every 15 s (e.g., the time interval of two consecutive track estimates used in the window test) as opposed to 3 s and the length of the sliding window is set to 4. It is shown that, in this case, the sliding window test has more power than the single time test.

The phenomenon that using more data may lead to lower power in the classical chi-square test seems counterintuitive. However, it can be better understood given the fact that the test uses only the likelihood function (LF) under H_0 and the LF under H_1 is unknown. Thus

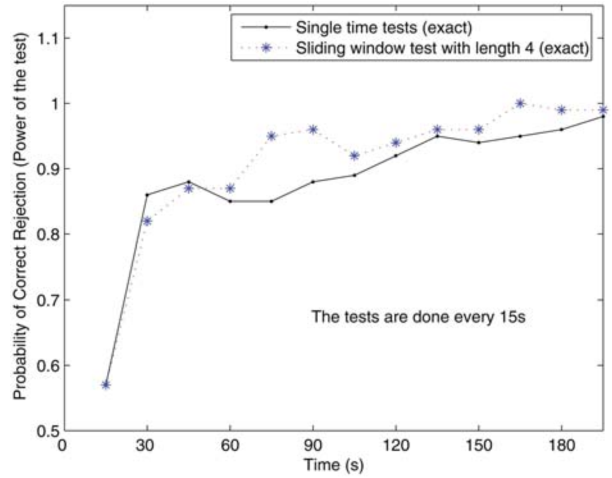

Fig. 13. Power of the test: sliding window test vs. single frame test with a increased testing interval of 15 s.

it is unclear how the available data should be combined to better differentiate the two hypothesis. The loss in power of the chi-square based window T2TA test is the result of the lack of information under H_1. A likelihood ratio (LR) test would be more powerful but it requires knowledge of the target separation, i.e., it is not practical.

6. CONCLUSIONS

In this paper the optimal T2TF algorithms at an arbitrary rate are investigated for various information configurations. First algorithms for T2TF without memory (T2TFwoM: fuser uses only the local track estimates at the fusion time) are presented for three information configurations, namely, T2TFwoM with no, partial and full information feedback. It is shown that, for T2TFwoM, information feedback is detrimental to fusion accuracy. Then algorithms for T2TF with memory (T2TFwM: fuser uses also the fused and local track estimates from the previous fusion) at an arbitrary rate are derived for information configurations with no, partial and full information feedback. It is shown that, at full rate, T2TFwM, with or without information feedback, is equivalent to the centralized measurement fusion (CMF, which is the global optimum). However, when operating at a lower rate, a certain amount of loss in fusion accuracy (compared to the CMF) is unavoidable. In contrast to the case of T2TFwoM, it is shown that information feedback improves the fusion accuracy of T2TFwM. And, unlike the information matrix fusion (IMF) which is optimal (same as CMF) only at full rate, the algorithms for T2TFwM are optimal at any rate.

An approximate implementation of the T2TF algorithms is also proposed based on the reconstruction of local information at the fusion center (FC). For nonlinear distributed tracking systems, it has much lower communication requirements and practically no loss in fusion accuracy due to the approximation. Simulation results show that it is consistent and, for the sensors-

[14] This is because with lower process noise the "memory" of the filter is "longer."

target geometry considered, it meets the performance bound of the centralized measurement fusion at the fusion points.

The hypothesis test for T2TA is also studied in this paper. The sliding window test for T2TA is presented. It uses track estimates in a time window and yields false alarm rates that match the theoretical values. The sliding window test was compared with the single time test and the results show that, counterintuitively, the sliding window test may have lower power than the single time test. This is because using more data also increases the degrees of freedom of the test statistics which has a negative impact on the power of the test. When the multiple frames of data selected for T2TA are strongly correlated, which happens for motion with low process noise, the increase in the noncentrality parameter is too small to overcome the negative effect of the increased degree of freedom. In such cases, the sliding window test may be counterproductive and has lower power than the single time test. In practice, this should be avoided by, e.g., increasing the time difference between the selected data frames.

REFERENCES

[1] Y. Bar-Shalom
On the track-to-track correlation problem.
IEEE Transactions on Automatic Control, **26**, 2 (Apr. 1981), 571–572.

[2] Y. Bar-Shalom
Update with out-of-sequence measurements in tracking: Exact solution.
IEEE Transactions on Aerospace and Electronic Systems, **38**, 3 (July 2002), 769–778.

[3] Y. Bar-Shalom
On hierarchical tracking for the real world.
IEEE Transactions on Aerospace and Electronic Systems, **42**, 3 (July 2006), 846–850.

[4] Y. Bar-Shalom
On the sequential track correlation algorithm in a multisensor data fusion system.
IEEE Transactions on Aerospace and Electronic Systems, **43**, 1 (Jan. 2008), 396.

[5] Y. Bar-Shalom and L. Campo
The effect of the common process noise on the two-sensor fused-track covariance.
IEEE Transactions on Aerospace and Electronic Systems, **22**, 6 (Nov. 1986), 803–804.

[6] Y. Bar-Shalom and X. R. Li
Multitarget-Multisensor Tracking: Principles and Techniques.
YBS Publishing, 1995.

[7] Y. Bar-Shalom, X. R. Li and T. Kirubarajan
Estimation with Applications to Tracking and Navigation: Algorithms and Software for Information Extraction.
Wiley, 2001.

[8] K. C. Chang, R. K. Saha, Y. Bar-Shalom and M. Alford
Performance evaluation of multisensor track-to-track fusion. In *Proceedings of 1996 IEEE/SICE/RSJ International Conference on Multisensor Fusion and Integration for Intelligent Systems*, Dec. 1996, 627–632.

[9] K. C. Chang, R. K. Saha, Y. Bar-Shalom
On optimal track-to-track fusion.
IEEE Transactions on Aerospace and Electronic Systems, **33**, 4 (Oct. 1997), 1271–1276.

[10] K. C. Chang, Z. Tian, and R. Saha
Performance evaluation of track fusion with information matrix filter.
IEEE Transactions on Aerospace and Electronic Systems, **38**, 2 (Apr. 2002), 455–466.

[11] H. Chen, T. Kirubarajan and Y. Bar-Shalom
Performance limits of track-to-track fusion vs. centralized estimation.
IEEE Transactions on Aerospace and Electronic Systems, **39**, 2 (Apr. 2003), 386–400.

[12] H. Chen and Y. Bar-Shalom
Track fusion with legacy track sources.
In *Proceedings of the 9th International Conference on Information Fusion*, Florence, Italy, July 2006.

[13] C. Y. Chong, S. Mori, and K. C. Chang
Distributed multitarget multisensor tracking.
In Y. Bar-Shalom (Ed.), *Multitarget-Multisensor Tracking: Advanced Applications*, MA: Artech House, 1990, ch. 8.

[14] D. K. Dey, N. Ravishanker
A First Course in Linear Model Theory.
Chapman & Hall/CRC, 2001.

[15] O. E. Drummond
A Hybrid sensor fusion algorithm architecture and tracklets.
In *Proceedings of 1997 SPIE Conference on Signal and Data Processing of small Targets*, vol. 3163, July 1997, 512–524.

[16] Y. He and J. W. Zhang
New track correlation algorithms in a multisensor data fusion system.
IEEE Transactions on Aerospace and Electronic Systems, bf 42, 4 (Oct. 2006), 1359–1371.

[17] X. R. Li and J. Wang
Unified optimal linear estimation fusion—Part II: Discussions and examples.
In *Proceedings of the Third International Conference on Information Fusion*, Paris, France, July 2000, MoC2.18–MoC2.25.

[18] X. R. Li, Y. M. Zhu, J. Wang and C. Z. Han
Unified optimal linear estimation fusion—Part I: Unified model and fusion rules.
IEEE Transactions on Information Theory, **49**, 9 (Sept. 2003), 2192–2207.

[19] X. R. Li and P. Zhang
Optimal linear estimation fusion—Part III: Crosscorrelation of local estimation errors.
In *Proceedings of the Fourth International Conference on Information Fusion*, Montreal, QC, Canada, Aug. 2001, WeB1.11–WeB1.18.

[20] X. R. Li and K. S. Zhang
Optimal linear estimation fusion—Part IV: Optimality and efficiency of distributed fusion.
In *Proceedings of the Fourth International Conference on Information Fusion*, Montreal, QC, Canada, Aug. 2001, WeB1.19–WeB1.26.

[21] X. R. Li, K. S. Zhang, J. Zhao, and Y. M. Zhu
Optimal linear estimation fusion—Part V: Relationships.
In *Proceedings of the Fifth International Conference on Information Fusion*, Annapolis, MD, July 2002, 497–504.

[22] X. R. Li
Optimal linear estimation fusion—Part VII: Dynamic systems.
In *Proceedings of the Sixth International Conference on Information Fusion*, Cairns, Australia, July 2003, 445–462.

[23] S. Mori, W. H. Barker, C. Y. Chong, and K. C. Chang
Track association and track fusion with nondeterministic target dynamics.
IEEE Transactions on Aerospace and Electronic Systems, **38**, 2 (Apr. 2002), 659–668.

[24] B. L. Scala and A. Farina
Effects of cross-covariance and resolution on track association.
In *Proceedings of the Third International Conference on Information Fusion*, vol. 2, Paris, France, July 2000, WED1/10–WED1/16.

[25] J. L. Speyer
Computation and transmission requirements for a decentralized linear-quadratic-Gaussian control problem.
IEEE Transactions on Automatic Control, **24**, 2 (Apr. 1979), 54–57.

[26] X. Tian and Y. Bar-Shalom
The exact algorithm for asynchronous track-to-track fusion.
In *Proceedings of SPIE Conference on Signal and Data Processing of small Targets*, Orlando, FL, Apr. 2010.

[27] K. S. Zhang, X. R. Li, P. Zhang, and H. F. Li
Optimal linear estimation fusion—Part VI: Sensor data compression.
In *Proceedings of the Sixth International Conference on Information Fusion*, Cairns, Australia, July 2003, 221–228.

[28] Chi-Square Distribution
http://en.wikipedia.org/wiki/Noncentral_chi-square_distribution.

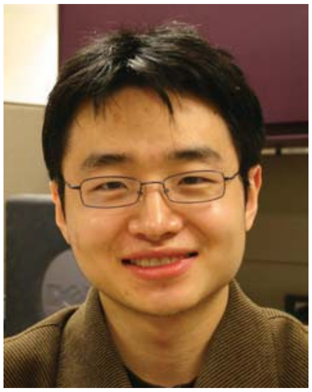

Xin Tian was born in 1980. He received the B.E. degree in 2002 and M.E. degree in 2005, both from the Department of Information and Communication Engineering, Xi'an Jiaotong University, China. He is now a Ph.D. candidate at the Department of Electrical and Computer Engineering, University of Connecticut.

His research interests include statistical signal processing, tracking and information fusion.

Yaakov Bar-Shalom was born on May 11, 1941. He received the B.S. and M.S. degrees from the Technion, Israel Institute of Technology, in 1963 and 1967 and the Ph.D. degree from Princeton University in 1970, all in electrical engineering.

From 1970 to 1976 he was with Systems Control, Inc., Palo Alto, CA. Currently he is Board of Trustees Distinguished Professor in the Dept. of Electrical and Computer Engineering and Marianne E. Klewin Professor in Engineering at the University of Connecticut. He is also Director of the ESP (Estimation and Signal Processing) Lab.

His current research interests are in estimation theory and target tracking and has published over 370 papers and book chapters in these areas and in stochastic adaptive control. He coauthored the monograph *Tracking and Data Association* (Academic Press, 1988), the graduate texts *Estimation and Tracking: Principles, Techniques and Software* (Artech House, 1993), *Estimation with Applications to Tracking and Navigation: Algorithms and Software for Information Extraction* (Wiley, 2001), the advanced graduate text *Multitarget-Multisensor Tracking: Principles and Techniques* (YBS Publishing, 1995), and edited the books *Multitarget-Multisensor Tracking: Applications and Advances* (Artech House, Vol. I, 1990; Vol. II, 1992; Vol. III, 2000).

He has been elected Fellow of IEEE for "contributions to the theory of stochastic systems and of multitarget tracking." He has been consulting to numerous companies and government agencies, and originated the series of Multitarget-Multisensor Tracking short courses offered via UCLA Extension, at Government Laboratories, private companies and overseas.

During 1976 and 1977 he served as Associate Editor of the IEEE Transactions on Automatic Control and from 1978 to 1981 as Associate Editor of Automatica. He was Program Chairman of the 1982 American Control Conference, General Chairman of the 1985 ACC, and Co-Chairman of the 1989 IEEE International Conference on Control and Applications. During 1983–87 he served as Chairman of the Conference Activities Board of the IEEE Control Systems Society and during 1987–89 was a member of the Board of Governors of the IEEE CSS. He was a member of the Board of Directors of the International Society of Information Fusion (1999–2004) and served as General Chairman of FUSION 2000, President of ISIF in 2000 and 2002 and Vice President for Publications in 2004–08.

In 1987 he received the IEEE CSS Distinguished Member Award. Since 1995 he is a Distinguished Lecturer of the IEEE AESS and has given numerous keynote addresses at major national and international conferences. He is corecipient of the M. Barry Carlton Award for the best paper in the IEEE Transactions on Aerospace and Electronic Systems in 1995 and 2000 and the 1998 University of Connecticut AAUP Excellence Award for Research. In 2002 he received the J. Mignona Data Fusion Award from the DoD JDL Data Fusion Group. He is a member of the Connecticut Academy of Science and Engineering. He is the recipient of the 2008 IEEE Dennis J. Picard Medal for Radar Technologies and Applications.